AE-497

UDC 532.5

AE-497

Effect of Wall Friction and Vortex Generation on Radial Void Distribution – The Wall – Vortex Effect

Z. Rouhani

AKTIEBOLAGET ATOMENERGI

STUDSVIK, NYKÖPING, SWEDEN 1974

EFFECT OF WALL FRICTION AND VORTEX GENERATION ON RADIAL VOID DISTRIBUTION - THE WALL-VORTEX EFFECT

by

Zia Rouhani

ABSTRACT

Arguments are presented to prove the existence of rolling vortices in two-phase flow. In liquid phase they will appear in a boundary layer near the walls while in the continuous vapor phase they will occur near the interface with a liquid film. The intensity and size of these vortices are expected to depend on the local velocity gradients normal to the walls. A discussion is given of the interaction between the rotational field associated with such vortices and bubbles in liquid flow or droplets in vapor flow. This interaction is called the wall-vortex effect. It appears that several, apparently unrelated, phenomena observed in two-phase flow systems may be interpreted in terms of this mechanism. Among these are:

- Radial void peaking near the walls
- Slip ratios less than unity observed even in vertical upward flow
- Reduced droplet diffusion near the liquid film
- Reduced vapor mixing between subchannels at low steam qualities
- Accelerated flashing process in flow of depressurized liquid

Finally, a comparison with the well-known Magnus effect is also included.

Printed and distributed in September 1974

LIST OF CONTENTS

1.	Introduction	3
2.	The structure of turbulent boundary layers	5
3.	The influence of different flow condition on the rolling vortices	8
4.	The Wall-vortex effect	9
5.	Formulation and estimation of the magnitude of local accelerations	12
	5.1 The order of magnitude of the dimensions and velocities	12
	5.2 Formulation of the acceleration components	14
	5.3 Numerical examples	16
6.	The influence of the Wall-vortex effect on two-phase mixing between subchannels	17
7.	The effect of wall-vortices on flashing of flowing depressurized liquid	19
8.	Conclusion	20
9.	References	21
	Appendix 1	23
	Figures	

1. INTRODUCTION

The complex picture of void distribution in two-phase flow will be familiar to any one who has glanced at a number of reports on this subject.

The complexity is not limited to the instantaneous pattern of distribution of the bubbles and droplets over the flow area, it also applies to the various distribution curves of time-averaged vapor volume fraction at different radial positions. However, the various distribution profiles are reproducable and, when carefully studied, they demonstrate a systematic dependence on mass velocity, average void and channel geometry.

In 1964 Staub and Zuber [1] reported radial void distribution data obtained during boiling of refrigerant -22 at relatively low mass velocities (G = 80 to 550 kg/m^2s) in a round tube of 10 mm inside diameter. These data immediately indicated that the local void fraction peaked near the walls at low qualities and that this local peaking increased with increasing mass velocity. Further data of this kind were subsequently reported by Kroeger and Zuber [2] in 1966. Shires and Riely [3] reported some data on radial void distribution in a round duct with air-water flow, obtained in connection with performance tests of the isokinetic sampling method.

Malnes [4] made systematic studies of radial void distribution both in air-water and in steam-water flow in round tubes. The air-water tests were performed with different tube diameters of 26.3 mm and 46 mm. The liquid velocities varied from 0.2 to 4 m/s. The interesting result of these studies was a series of diagrams which indicated a definite occurence of the peaking of air bubbles near the tube walls, at

low values of average void, and the increase in this tendency with increasing liquid velocity. Figures 1 and 2 represent two comparison cases with measured profiles taken from the material in ref [4] (with the kind permission of Dr Dag Malnes of IFA, Kjeller, Norway).

The diagrams show that the peak value of the local voids appears at a small distance from the wall and that the peaking is influenced by the average liquid velocity.

Of particular interest, in this connection, is the fact that repeated measurements at two different heights in the test section showed almost no reduction in the void peaking near the walls. In some of the runs it was even possible to see a sharpening of the peaks at the upper level. Two typical cases of this kind are reproduced from ref [4] in Fig 3.

Further data on radial void distribution are reported by Staub and Walmet [5], Shiralkar [6] and Dix [7]. All of these data demonstrate a similar trend.

A review of the published data of this kind gives a confirmed impression that, in addition to process by which the bubbles are generated at the wall, there must be another mechanism which maintains most of the bubbles at a certain distance from the wall as opposed to their being exactly at the wall surface.

In the literature dealing with void calculations there is very little available that concerns radial void profiles. Kroeger and Zuber [2] suggested a power function of the relative radial position which was a direct fitting of their own data. No phenomenological explanation was given. The power law formula would lead to erronious predictions of void fraction at the wall if applied to the data of ref [4].

J S Skaug [8] presented a qualitative explanation on the basis of local hydrostatic pressure differences and the operation on the bubbles of a lateral force due to their relative upwards velocity within a liquid

velocity gradient. It seems that the possibility of including the effect of friction and vortex generation on void distribution has been completely ignored.

In this report attention is paid to the general phenomenon of vortex generation near the solid walls. This will be first discussed in the case of single-phase flow and then extended to two-phase flow systems. Particularly interesting aspects in two-phase flow are provided by the concentration near the solid walls of bubbles in rolling liquid vortices and the dissipation near the interface with a liquid film of liquid droplets from these same vortices.

The practical importance of these considerations relates to several aspects of two-phase flow as will be described later.

The effect of rolling vortices on the radial distribution of vapor and liquids is quite different from the well known Magnus effect as will be explained in the Appendix.

2. THE STRUCTURE OF TURBULENT BOUNDARY LAYERS

To provide a proper foundation for the arguments to be presented concerning the mechanisms that influence the structure of two-phase flow it seems useful to recite some of the relevant studies of the structure of turbulent boundary layers.

Although the amount of work published on the subject of turbulent boundary layer is very great, the number of articles dealing with the actual structure of the boundary layer is rather limited. In almost all of the published work the experimental and theoretical studies of the turbulent boundary layer have been made on the basis of the classical approach whereby the local velocities, in different directions are represented as a time-averaged value on which is superimposed a fluctuat-

ing component. The literature contains elaborate mathematical treatments of the velocity distribution, based either on the phenomenological concept of mixing length theory [9 and 10] or, on a purely statistical treatment of the fluctuations [10]. Although very useful in providing accurate predictions of the average velocity profiles, an approach of this type yields no information on the actual mechanism of turbulence generation, nor does it indicate the pattern of motion of the fluid particles within the turbulent layer.

Of particular interest to the present discussion is the visual observation of flow behaviour within the turbulent boundary layer. Two noticeable examples of this type of study will be mentioned here. One source is the relatively old information available from H Schlichting's book on Boundary Layer Theory [9] where reference is made to the studies reported by Nikuradse. In this work pictures were taken, with a moving camera, of the turbulent liquid flow in an open channel. By varying the relative velocity of the camera it was possible to obtain pictures that clearly showed the different stages of formation and movement of the rolling vortices which were seen to form near the solid walls and then move into the main stream.

Another work which is of interest in this connection is an article on the structure of turbulent boundary layers by S J Kline et al [11]. In this work the authors present a considerable amount of material and argument, based on measurements and visual studies of various velocity components within the boundary layer, which support the concept of the formation of rolling vortices near the walls.

They refer to a model suggested by Lighthill [12] who considered the existence of a turning process within the boundary layer. The rolling vortices are called wall-layer streaks and Kline et al derived a relationship between the frequency of breakup, average spacing of these

streaks (or vortex filaments) and the shear velocity, expressed as

$$\omega^+ = 2\pi F^+ \lambda^+ \cong 0.06 \ (\text{sec}^{-1}) \tag{1}$$

where

$$F^+ = F\nu^2/u_\tau^3 \tag{2}$$

F = frequency of streak breakup per unit span

$$\lambda^+ = \lambda \, u_\tau/\nu \tag{3}$$

λ = visually observed, mean spacing of streaks. u_τ = the shear velocity determined from the velocity slop at the wall. ν = kinematic viscosity.

From the experimental data of ref [11] an average value of λ^+ = 100 is suggested.

Although the general pattern of the turbulent boundary layer may be somewhat chaotic and shapeless, one may still expect that there will be a dominance of rotational motion in a certain direction. This will be dictated by the upply of linear momentum, donated by the fluid particles which enter from the main flow, and the decelerating effect of viscosity in the viscous sublayer. Figure 4 is a schematic representation showing the motion of the vortices near the walls and the path of one particle on the periphery of such a vortex.

In conclusion to this introductory discussion it may be said that the existence of rolling vortices within and in the vicinity of the boundary layer near the solid walls is a proven phenomenon and a feature of turbulent flow. It then remains to examine the extent of this mechanism in two-phase flow and to evaluate the interaction of the rolling liquid vortices with bubbles or that of the rolling vapor vortices with liquid droplets.

3. THE INFLUENCE OF DIFFERENT FLOW CONDITIONS ON THE ROLLING VORTICES

In single-phase flow the thickness of the viscous sublayer and that of the so-called buffer layer will be affected by kinetic viscosity and the velocity of flow. A mathematical relationship between these factors is given in the universal velocity distribution law [9 and 10]. According to this law the thickness of various layers decreases with decreasing kinematic viscosity and with increasing velocity. In terms of vortex generation on the walls this may be interpreted as a decrease in the average diameter of rolling vortices with decreasing viscocity or increasing velocity. This interpretation fits the general observation that, in turbulent flow, the friction factor decreases with increasing Reynolds number. One may visualize a train of rolling vortices within the boundary layer. These will cause a continuous exchange of mass between a zone with a very low velocity and the main flow which has a high velocity. The extent of momentum exchange will decrease as the average size of the vortices decreases.

It may be said that the rolling vortices are produced by the torque due to the linear momentum of the fluid particles, which are linked through viscosity to the low velocity zone in the laminar sublayer. The size of these vortices will depend on the torque and the viscosity and will, in turn, control the rate at which flow momentum is dissipated to the laminar sublayer.

In two-phase flow the presence of bubbles or droplets will clearly have an additional effect on the size of the rolling vortices. The presence of particles within the flow will increase the size of the vortex streaks and accordingly produce an increased rate of momentum dissipation from the main flow to the viscous sublayer.

Large-sized rolling vortices in two-phase flow are seen to originate quite simply due to the interaction of rotational fields with density differences of the two phases as described in greater detail in the following section.

4. THE WALL-VORTEX EFFECT

There is clearly a field of centrifugal acceleration within and around each rolling vortex that is close to the conduit wall. If there are any particles or bubbles present in the flow they will be subject to a force of either repulsion or attraction with respect to the center-line of the nearest vortex. This may be called a wall-vortex effect. (Although even a local obstacle in the flow may generate vortices which will have similar effects.) The direction of the centrifugal or centripetal force will, naturally, depend on the relative density of the immersed particle. In the case of bubbles in liquid flow, the acting forces will be centripetal and will tend to collect the bubbles on the center-lines of the vortex streaks. But, within the vapor vortices, produced close to the interface with a liquid film, the liquid droplets will be thrown away from the centres of rotation by the associated forces.

In the case of liquid flow with bubbles, one may expect that, at least, some of the bubbles will form centers of rotation for a layer of surrounding liquid. In addition to its dependence on flow velocity, which generates a torque, the size of the rolling vortices must also depend on the bubble concentration in the flow and on the physical properties which govern the size of the bubbles. This view is supported by the experimental data reported in refs [1] to [7].

If this explanation is true one may conclude that the average motion of the bubbles within the rolling vortices will be strongly influenced

by wall friction. Although unattached to the solid walls, these bubbles will not be free to attain a rising velocity owing to the normal influence of gravity. This conclusion is also in agreement with many experimental data which show that, even in a vertical upward flow, slip ratios less than unity have been observed at low void fractions. Of particular interest in this respect are the data on air-water experiments reported by Malnes [4]. In a system of this kind the less-than-unity slip ratios cannot be related to the fixation of some bubbles on the walls. However, the presence of bubbles within the wall-vortex layer will contribute to the buoyancy of the whole layer.

As the population of bubbles in liquid flow increases the average size of the rolling vortices will also increase due to aglomoration of the concentrated bubbles. But after a certain limit has been reached the liquid phase will become discontinuous. At this stage the organized field of forces which retained the bubbles close to the walls will vanish. The mechanism of vortex generation on the walls will be very irregular and the radial void distribution will become flat. The onset of this stage will depend on the shape of flow area and its wall-to-wall dimensions compared with the average bubble diameter. With further increase in vapor flow a regular pattern of rolling vortices may appear within the continuous vapor phase, moving close to the interface with a liquid film on the conduit wall. These vapor vortices will also generate a field of centrifugal forces. This will act on the liquid droplets tending to throw them either onto the liquid film or into the vapor core. At sufficiently high vapor velocities, which are expected to produce strong rotations, it should be possible to detect a zone of relatively low droplet concentration near the interface with the liquid film. This zone will correspond to the loci of the center lines of the rolling vortices.

Such a tendency is indeed detectable according to the data reported by L B Cousins and G F Hewitt [13]. Figures 5 and 6 (reproduced from ref [13] by the authors' kind permission) show a minimum in the local water mass velocities at relative radial distances of 0.42 and 0.20 from the wall. The reported data clearly demonstrate the influence of increased rate of gas flow on the reduction of the local droplet concentration and a shifting of this region closer to the film interface.

The same set of data lend additional support to the concept of the wall-vortex effect on the basis of the measured rates of droplet diffusion across the channel.

If, as speculated here, the rolling vortices are generated and move within the vapor phase in a zone close to the interface, they can be expected to act as a partial barrier to smaller droplets (owing to the associated centrifugal effect) thus hampering the diffusion of droplets between the liquid film and the vapor core. This explanation is in good agreement with the reported data. Figures 7 and 8 (reproduced from ref [13]) show the minima of dye and droplet diffusion coefficients in a zone near the interface with the liquid film. The interesting fact is that, according to the data, the depression in the diffusion coefficients becomes more pronounced as the rate of air flow increases. Obviously the centrifugal effect of the vapor vortices would increase with the flow rate of this phase.

Finally, consideration can be given to the local flow pattern within the liquid film and study this in terms of the occurrence of rolling vortices. If the film is so thin that it matches the thickness of a laminar layer sufficient to support the whole friction force, the velocity distribution in the film can be assumed to be linear and in that case there will be no possibility for the formation of rolling vortices.

The flow pattern in a thick film may, however, be a combination of laminar flow in a very thin layer near the solid wall and a system of rolling vortices in contect with the vapor (interface).

In this event, some smaller bubbles may become confined to the liquid film if it is sufficiently thick, as a result of their attraction to the center lines of the vortex filmaments. Such bubbles may originate either in boiling on the wall or overlapping of the rolling waves on the interface (or both). The population of these bubbles will be governed by the rate of their generation and the statistical chances of destruction of the rolling vortices which carry them.

5. FORMULATION AND ESTIMATION OF THE MAGNITUDE OF LOCAL ACCELERATIONS

To give some impression of the magnitude of the forces developed due to the wall-vortex effect some rough calculations will be performed in the following section.

5.1. The order of magnitude of the dimensions and velocities

Since the wall-vortex effect has hitherto passed unnoticed as a phenomenon no measurements are available for consideration. Accordingly, there is no direct information as regards the loci of the center lines of the rolling vortices and their average distance from the wall under different conditions. It thus becomes necessary to resort to some other type of information to obtain an indirect estimation of the average distance of the vortex centres from the wall.

In this connection use can be made of the measured void profiles, treating them in accordance with the arguments presented here. The results demonstrate that the position of the center lines of the rolling

vortices coincide with the measured peaks of raidal void distribution.

As an example, use will be made of run no 358 of ref [4], the void profile being that shown in Fig 2. According to the data the average distance of the peaks from the wall is about $\delta_b \cong 2.8$ mm.

The thickness of the viscous sublayer will be obtained from the universal velocity distribution law. According to this the non-dimensional distance from the wall at the outer edge of the viscous sublayer is about 5.5 [10].

$$y^+ = \delta_v v_* / \nu = 5.5$$

or, using the definition of the shear velocity, v_*

$$\delta_v = 5.5 \cdot \nu \sqrt{\frac{1}{8} f \bar{U}_1^2}$$

In this equation f is the friction factor for which we use the measured value for two-phase flow, namely $\lambda_{TP} \cong 0.045$ [4]. This gives (with ν for water)

$$\delta_v = 0.1 \text{ mm}.$$

The local axial velocity at the edge of the visous sublayer will be (again according to the universal law)

$$U^+ = U_v / v_* = U_v / (\frac{1}{8} f \bar{U}_1^2)^{0.5} = 5.5$$

This gives

$$U_v = 0.412 \, \bar{U}_1 = 0.32 \text{ m/s}$$

It may be assumed that the average velocity of the rolling vortices along the wall will be the mean value between the bulk liquid

velocity and U_v. Hence, the effect of buoyancy of the bubble layer being neglected here,

$$V_c = 0.5\ (\bar{U}_1 + U_v) = 0.5\ (.776 + .32) = 0.458\ \text{m/s}$$

The relative velocity of the vortex centers with the edge of the viscous sublayer will thus be

$$V_r = V_c - U_v = 0.548 - 0.32 = 0.228\ \text{m/s}$$

This will correspond to the "wheeling" velocity of the rolling vortices (or of the liquid layer around the bubbles).

5.2. Formulation of the accleration components

The absolute velocity of a fluid particle on the periphery of this vortex will have the following components (with respect to the tube wall)

$$V_a = V_c + V_r \cos\omega \tag{4}$$

in the axial direction and

$$V_n = V_r \sin\omega \tag{5}$$

normal to the wall.

In these equations ω is the angular position measured from the point on the vortex circle which is tangent to the main stream as shown in Fig 4. Hence

$$\frac{d\omega}{dt} = \frac{V_r}{0.5\ (\delta_b - \delta_v)} \tag{6}$$

(V_r, δ_b and δ_v were defined in 5.1).

The total acceleration vector developed by the particle motion will be

$$\vec{a} = \frac{W^2}{R_m} \vec{n} + \frac{dW}{dt} \cdot \vec{u} \tag{7}$$

in which $W = \sqrt{V_a^2 + V_n^2}$ and R_m is the local radius of curvature of the particle path in space.

The first term on the right hand side gives the local centrifugal acceleration and $\vec{n}$ is a unit vector in the radial direction (along R_m). The second term is the tangential acceleration and $\vec{u}$ is a unit vector in this direction.

After performing the necessary mathematical operations one obtains the following relationship.

For the centrifugal part of the acceleration

$$\Omega = \frac{W^2}{R_m} \equiv \frac{V_r^2}{\delta_b - \delta_v} \tag{8}$$

and for the tangential part

$$\frac{dW}{dt} = \frac{1}{W} (V_n \cos\omega - V_a \sin\omega) \frac{V_r^2}{\delta_b - \delta_v} \tag{9}$$

Of these the acceleration term Ω will always act along a radius away from the center of the vortex, but the second term $\frac{dW}{dt}$ will vary in size and direction.

The alternating acceleration vector $\frac{dW}{dt} \vec{u}$ may be resolved into two components, one of which is parallel with the solid wall and one normal to the wall. It can be shown that the time average of the acceleration component parallel to the wall will be zero, when the vortex has completed a rotation. The normal component, however, will generally assume a positive value and always be directed away from the solid wall. The maximum value of this component will appear when $\omega = 120^\circ$ or

$\omega = 240^{\circ}$. At these positions the magnitude of the normal-to-the wall acceleration component will be 0.414Ω. (The minimum value, which is zero, occurs at $\omega = 180^{\circ}$ and 360°.)

The net result of the normal-to-the wall component of the acceleration will resemble a gravitational force that pushes the heavier medium (liquid) away from the wall causing the bubbles to drift towards it. At the same time the centrifugal acceleration component will acet in such a way as to keep the bubbles concentric with the rolling vortices.

5.3. Numerical examples

With reference to the numerical values which were estimated (in part 5.1) for δ_b, δ_v and V_r use of the preceeding equations yields the following results.

For the centrifugal acceleration

$$\Omega = V_r^2/(\delta_b - \delta_v) = 0.228^2/0.0027 = 19.25 \text{ m/s}^2$$

and for the normal-to-the wall component

$$\overline{\frac{dW}{dt}} \simeq \frac{1}{2}\, 0.414\Omega = 3.985 \text{ m/s}^2$$

The centrifugal acceleration is thus seen to be almost twice that of normal gravity, g, although it is the result of a relatively low flow velocity ($U_1 = 0.6$ m/s). It should be remembered that these accelerations increase quadratically with the flow velocity.

If the above calculations are repeated for the case of $U_1 = 1.5$ m/s, taking into consideration the reduction in δ_b, as indicated by the data on run no 364 in Fig 2, the following results are obtained.

$$\Omega = 293.5 \text{ m/s}^2 \cong 30 \text{ g}$$

and

$$\overline{\frac{dW}{dt}} \cong \frac{1}{2} 0.414\Omega = 60.75 \text{ m/s}^2 \cong 6.2 \text{ g}$$

A bubble within the liquid mass subject to this acceleration field will not be free to rise, under the influence of natural gravity, even if it happens to be at the lower surface of a horizontal tube.

The average axial velocity of the layer that includes the rolling vortices will be less than the mean flow velocity. According to the rough calculations performed for the above mentioned cases the axial velocity of these layers is expected to be 0.548 m/s in the first case and 1.274 in the second. Both values are less than average liquid velocities. Hence, as far as these layers are concerned, the gas phase has an upward velocity which is less than that of the liquid phase. However, the average gas velocity over the channel area as a whole will be higher, due partly to the rising velocity of the bubbles outside of the boundary layer and partly to the extra buoyancy of the boundary layer.

One consequence of this effect is that slip ratios less than unity are to be expected at low void fraction and high liquid velocity. Fig 9 which is further extract from ref [4] supports this conclusion. Furhtermore, slip ratios calculated from the data given by Staub and Wamlet [5] yield values less than unity at low steam qualities.

6. THE INFLUENCE OF THE WALL-VORTEX EFFECT ON TWO-PHASE MIXING BETWEEN SUBCHANNELS

Repeated experiments performed on mixing between subchannels in two-phase flow have consistently posed a dilema; the vapor phase mixing decreases with increasing liquid velocity while the liquid phase

mixing improves with velocity. Experimental evidence of these observations are reported by D S Rowe and C W Angle [14], T van der Rose [15] and K F Rudzinski et al [16].

Before any attempt is made to explain the effect of rolling vortices on vapor mixing it should be pointed out that the relatively low rate of vapor mixing is observed only in the bubble flow regime. The mixing rate improves considerably when the flow regime is changed to slug flow and particularly at the transition to annular flow [16]. Another point that must be observed is the distinction between vapor mixing and diversion cross-flow namely that the latter increases with the onset of steam generation in one subchannel.

It has already been stated that when the liquid phase is continuous the rolling vortices near the walls can be expected to arrest many of the bubbles. The intensity of vortex generation and the rotational speed should be strongest at the positions of highest velocity gradient normal to the walls. The cross-sectional view of the common types of subchannel and the typical patterns of velocity distribution in those subchannels, are shown in Fig 10. Consideration of this diagram indicates that, except in the case of the corner subchannel with an annular shape, the strongest velocity gradients will occur at positions remote from the gaps. It then follows that the vapor bubbles will be rather isolated from the path of flow mixing and hence vapor mixing will be poor in bubble flow regime with the exception of such exchanges as occur between a corner subchannel of annular shape and a side subchannel. According to this explanation the effect of vapor mixing in the latter instance should be rather one sided (owing to a relatively higher contribution by the vapor in the corner subchannel). Unfortunately, this particular test geometry has not been studied in any one of the reported mixing experiments.

With this argument as a basis it is evident that a relevant method

of mixing calculation in two-phase flow must, in addition to the effect of flow regime, also include a representation of the subchannel geometry and the factors which influence the radial velocity gradients. The ordinary concept of equivalent hydraulic diameter will not be an adequate description of the geometry in this case.

7. THE EFFECT OF WALL VORTICES ON FLASHING OF FLOWING DEPRESSURIZED LIQUID

According to J Flinta [17] projecting obstacles in the discharge line for depressurized water appear to reduce the delay time to the onset of flashing.

This particular effect could be considered as a result of flow separation behind the obstacle since such a separation would cause cavitation and initiate flashing.

However, once the nucleation of flashing bubbles has taken place, the rolling wall vortices will exert an influence by supressing the effect of surface tension, and accelerating the flashing process, within the turbulent boundary layer. The limiting factor in this process will be the thermal conductivity of the liquid phase.

In this connection an estimate of the local pressure, within a bubble at the center of a rolling liquid vertex, may be of some interest.

If it is assumed that the angular velocity is uniform within each vortex, that is to say, from its outer radius R to the bubble radius r_b, then the relationship between the static pressures, p_b in the bubble and p_1 in the bulk liquid flow will be

$$p_b = p_1 + 2\sigma/r_b - \rho_1(R - r_b)V_r^2/R$$

where σ is the surface tension, ρ_1 is the liquid density, and V_r is the "wheeling" speed of the rolling vortex as defined in part 5.

The third term on the right-hand side of the above equation shows the effect of wall vortex on reducing bubble pressure. This will be equivalent to a reduction in the amount of liquid superheat required for the continuation of flashing. It should be noted that the effect of this term will be gained separately from the results of depressurization due to the linear acceleration of the liquid.

The above argument leads to the following observations.

a. The rate of flashing will depend on the initial liquid velocity

b. The rate of flashing will depend on the ratio of wetted perimiter to flow area. In the case of flashing, which occurs inside round ducts, the process is expected to be faster in tubes with smaller diameters under equivalent conditions.

8. CONCLUSION

As stated in the summary given at the beginning of this account, the wall-vortex effect seems to explain several pecularities observed in two-phase flow. Among these are

- Radial void peaking near the wall
- Slip ratios less than unity observed even under conditions of vertical upward flow
- Reduced droplet diffusion near the liquid film
- Reduced vapor mixing between subchannels at low steam quality
- Accelerated flashing process in a flow of depressurized liquid

The intensity and size of the rolling wall vortices will depend on the local velocity gradients normal to the walls. Hence a proper formulation of mathematical models to permit calculation of the above mentioned behaviour must be based on those physical factors which influence the transverse velocity gradients.

9. REFERENCES

1. STAUB F W and ZUBER N,
A program of two-phase flow investigation: Fifth quarterly report. 1964.
(GEAP-4631).

2. KROEGER P G and ZUBER N,
A program of two-phase flow investigation: Thirteenth quarterly report. 1966.
(GEAP-5203).

3. SHIRES G L and RILEY P J,
The measurement of radial voidage distribution in two-phase flow by isokinetic sampling. 1966.
(AEEW-M650).

4. MALNES D,
Slip ratios and friction factors in the bubble flow regime in vertical tubes.
KR-110.

5. STAUB F W and WALMET G E,
Heat transfer and hydraulics: the effects of subcooled voids.
NYO-3679-8 (EURAEC-2120), (May 1969).

6. SHIRALKAR B S,
Local void fraction measurements in freon-114 with a hot-wire anemometer. General Electric Co. 1970.
NEDE-13158.

7. DIX G E,
Vapor void fractions for forced convection with subcooled boiling at low flow rates. 1971.
(NEDO-10491).

8. SKAUG J S,
Effects governing the shape of the void profile in bubble flow.
Institutt for Atomenergi, Kjeller, Norway 1968.
(Internal report RT-59).

9. SCHLICHTING H,
Boundary layer theory.
McGraw-Hill New York 1960.

10. BRODKEY R S,
The phenomena of fluid motions.
Addison-Wesley Publishing Co Reading Mass 1967.

11. KLINE S J, REYNOLDS W C, SCHRAUB F A and RUNSTADLER P W,
The structure of turbulent boundary layers.
J Fluid Mech 30 (1967) p 741.

12. LIGHTHILL M J,
Laminar boundary layers. Ed by L Rosenhead.
Clarendon Press, Oxford 1963, p 99.

13. COUSINS L B and HEWITT G F,
Liquid phase mass transfer in annular two-phase flow: radial liquid mixing. 1968.
(AERE-R 5693).

14. ROWE D S and ANGLE C W,
Cross-flow mixing between parallel flow channels during boiling. Part III, effect of spacers on mixing between two channels. 1969.
(BNWL-371) Pt 3.

15. VAN DER POS T,
On two-phase flow exchange between interacting hydraulic channels. 1970.
(WW015-R160).

16. RUDZINSKI K F, SINGH K and ST PIERRE C C,
Turbulent mixing for air-water flows in simulated rod bundle geometries.
Can J Chem Eng 50 (1972):2 p 297.

17. FLINTA J F,
Private communication.
AB Atomenergi, Studsvik, Nyköping, Sweden.

18. SEGRE G and SILBERBERG A,
Behaviour of macroscopic rigid spheres in Poiseuille flow. Parts 1 and 2.
J Fluid Mech 14 (1962) p 115 and p 136.

19. EICHHORN R and SMALL S,
Experiments on lift and drag of spheres suspended in a Poiseuille flow.
J Fluid Mech 20 (1964) p 513.

20. JEFFREY R C and PEARSON J R A,
Particle motion in laminar vertical tube flow.
J Fluid Mech 22 (1965) p 721.

21. OLIVER D R,
Influence of particle rotation on radial migration in the Poiseuille flow of suspensions.
Nature 194 (1962) p 1269.

22. SWANSON W M,
The Magnus effect: A summary of the investigations to date.
J Basic Eng 83 (1961) p 461.

APPENDIX 1

The Magnus Effect and How it Differs from the Wall-Vortex Effect

In the literature on suspension flows there are many reports devoted to theoretical and experimental studies of the behaviour of solid particles in a flow through a tube. Among the works referred to are those of Segre and Silberger [18], R Eichron and S Small [19], and R Jeffrey and J R A Pearrson [20]. These studies are almost entirely limited to the behaviour of particles in laminar flow. It has been generally observed [20] that in laminar flow dense particles falling slowly through a rising body of fluid migrate to the tube axis; buoyant particles in the same flow migrate to the tube wall. Conversely, dense particles falling through a descending fluid migrate to the tube walls and buoyant particles to the tube axis. D R Oliver [21] observed that the radial movement of suspended spheres in a laminar flow was dependent upon their rotational spin and explained this pehnomenon in terms of the Magnus effect.

The Magnus effect is well described by W M Swanson [22]. In the introduction to his article Swanson describes the Magnus effect in the following terms; "A spinning missile or body travelling through the air, in such a way that the body axis of rotation is at an angle with the flight path, will experience a Magnus force component in a direction prependicular to the plane in which the flight path and rotational axis lie".

Clearly, the relative axial velocity of a buoyant or dense particle, within the field of velocity gradient of a laminar flow inside a tube, may generate some rotation. This rotation can, in turn, be expected to develop a Magnus force which will impart a radial motion to the particle until the force is balanced by some other effect.

It should be observed that the Magnus effect is a result of the interaction of the spinning motion of a moving body with its translational motion in a medium. This is an entirely different effect from that produced by the influence of a centripetal or centrifugal force on a particle within the rotational field of a vortex. In some cases, however, the motion of suspended particles may be the result of an addition of both of these effects.

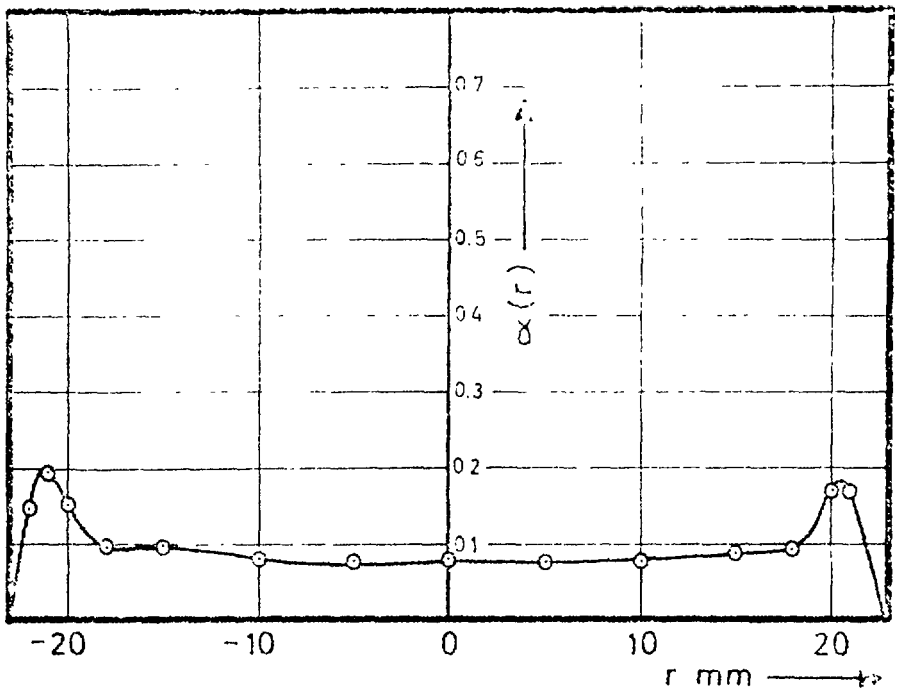

VOID PROFILE, 46 mm, $U_l = 0.6$ m/s, $\alpha = 0.102$, RUN 357

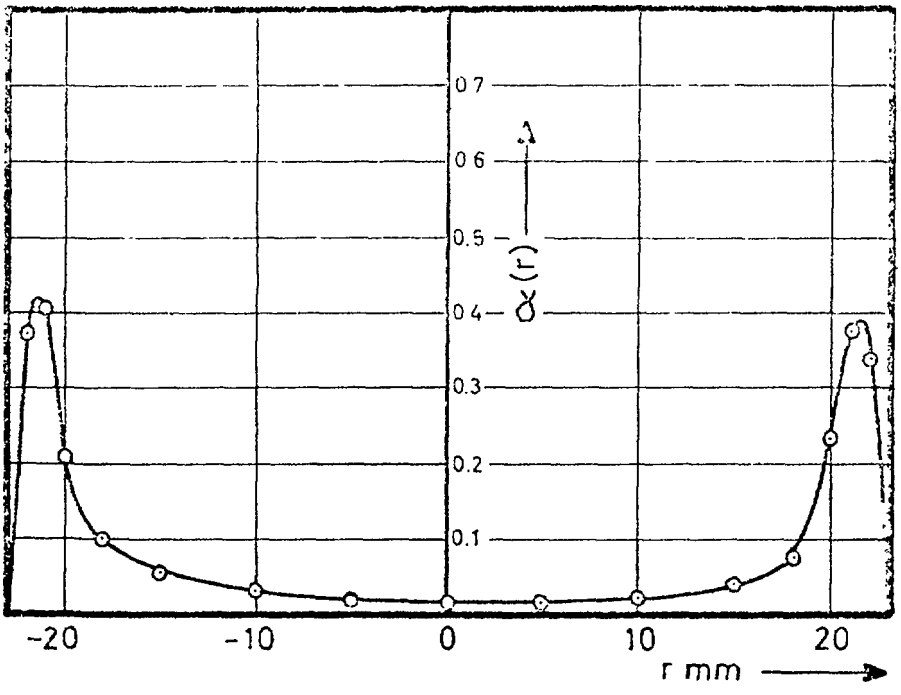

VOID PROFILE, 46 mm, $U_l = 1.5$ m/s, $\alpha = 0.11$, RUN 363

Fig 1. Comparison of two cases of radial void distribution in air-water flow, with roughly the same average void but different liquid velocities. Data reported by D Malnes. (Reproduced from ref [4] by permission.)

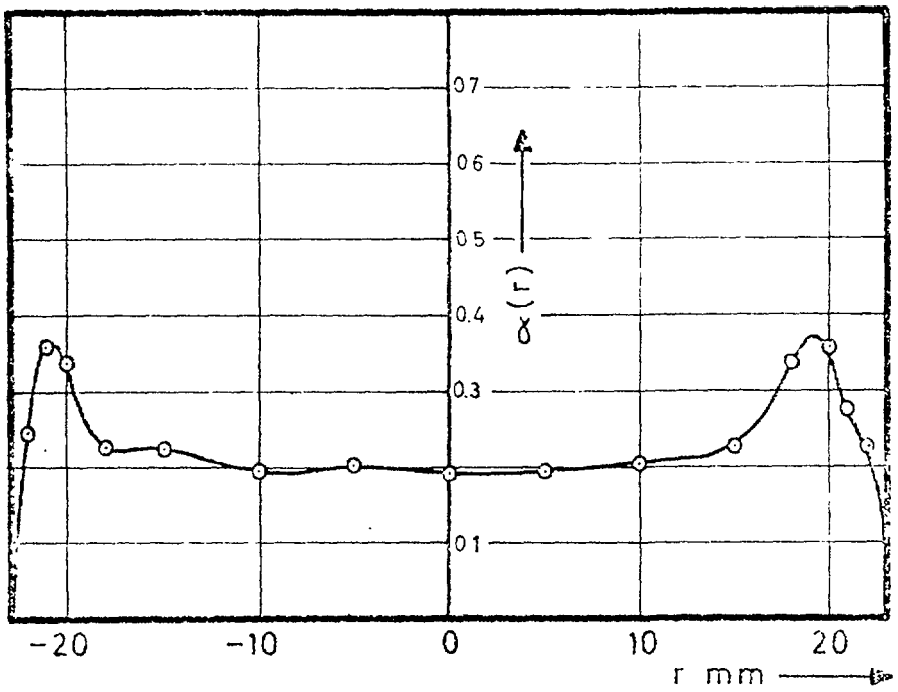

VOID PROFILE, 46 mm, $U_l = 0.6$ m/s, $\alpha = 0.227$, RUN 358

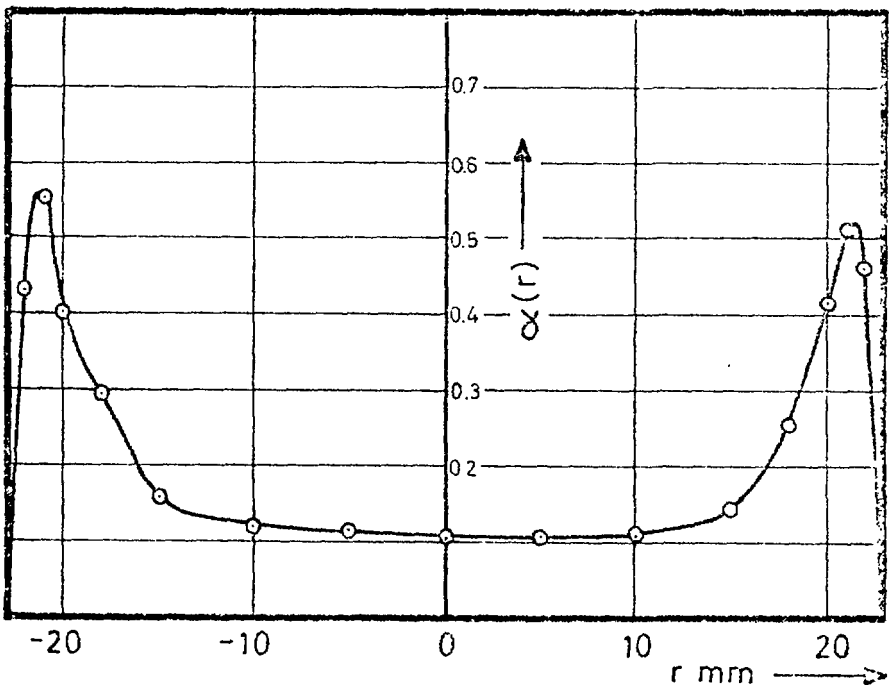

VOID PROFILE, 46 mm, $U_l = 1.5$ m/s, $\alpha = 0.23$, RUN 364

Fig 2. Comparison of two cases of radial void distribution in air-water flow, with roughly the same average void but different liquid velocities. Data reported by D Malnes. (Reproduced from ref [4] by permission.)

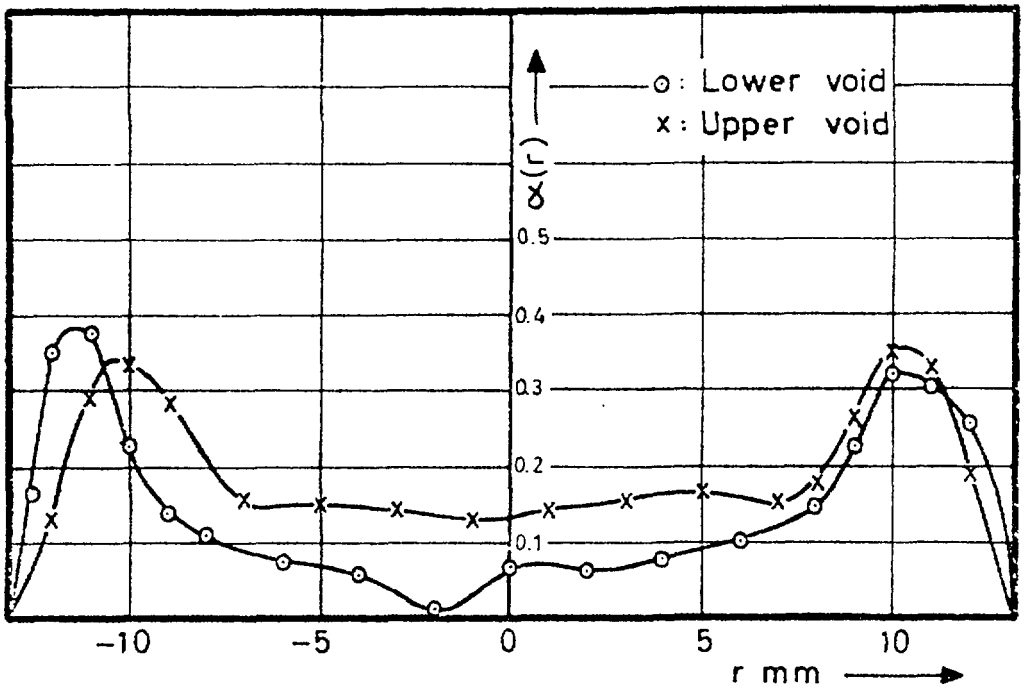

VOID PROFILES, 26.3 mm, U_l= 1.0 m/s, α = 0.201, RUN 340

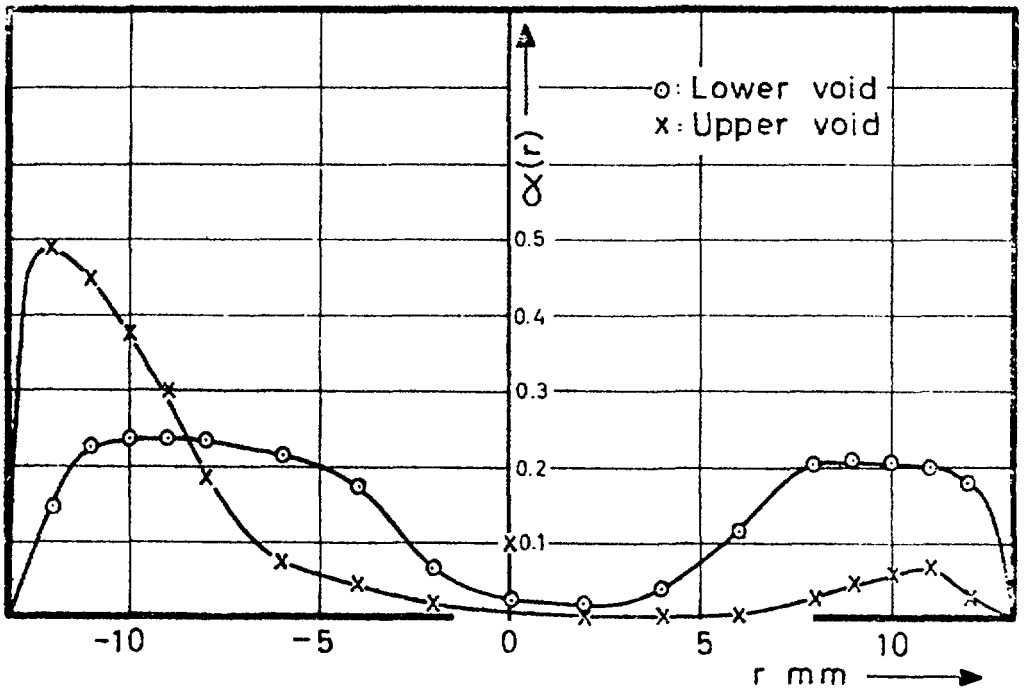

VOID PROFILES, 26.3 mm, U_l= 2.0 m/s , α = 0.159 , RUN 355

Fig 3. A demonstration of the stability of the radial void peaking near the walls. Data reported by D Malnes. (Reproduced from ref [4] by permission.)

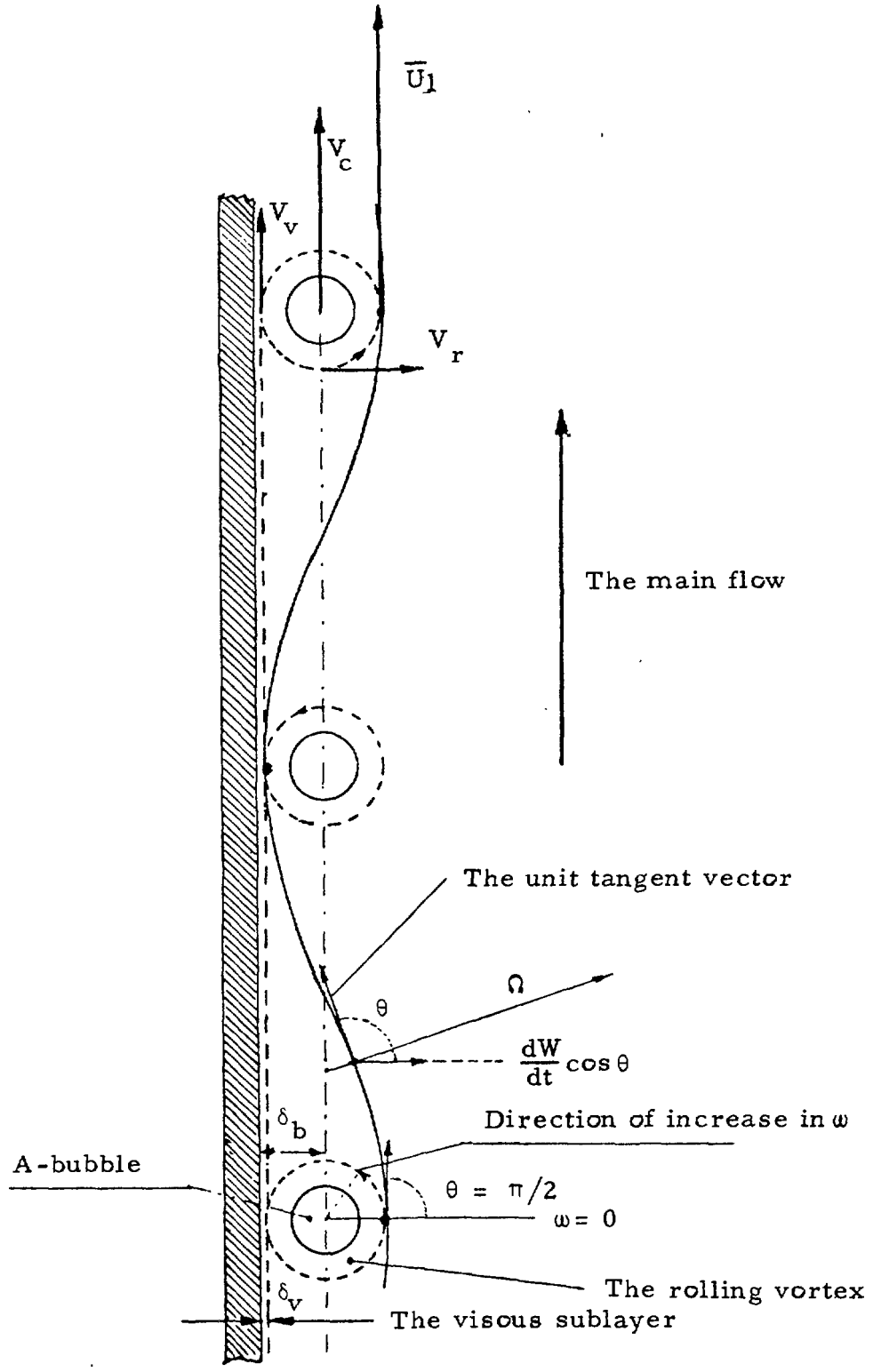

Fig 4. The idealized path of a fluid particle on the periphery of a wall vortex rolling in contact with the viscous sublayer.

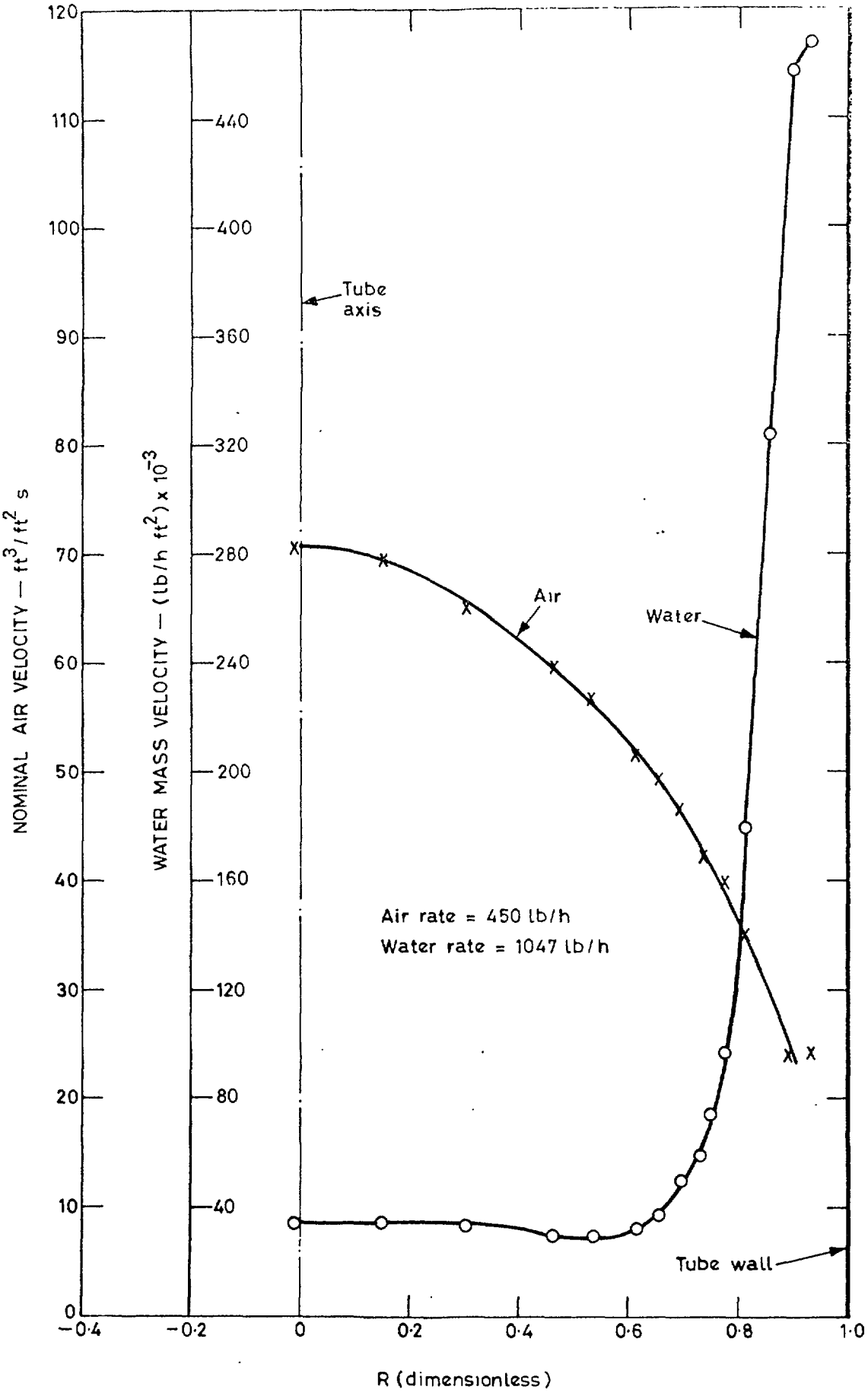

Fig 5. Mass velocity profiles obtained by the use of the isokinetic sampling prob. Data by Cousins and Hewitt (reproduced from ref [13] by permission). The liquid mass velocity shows a minimum in the vicinity of the interface.

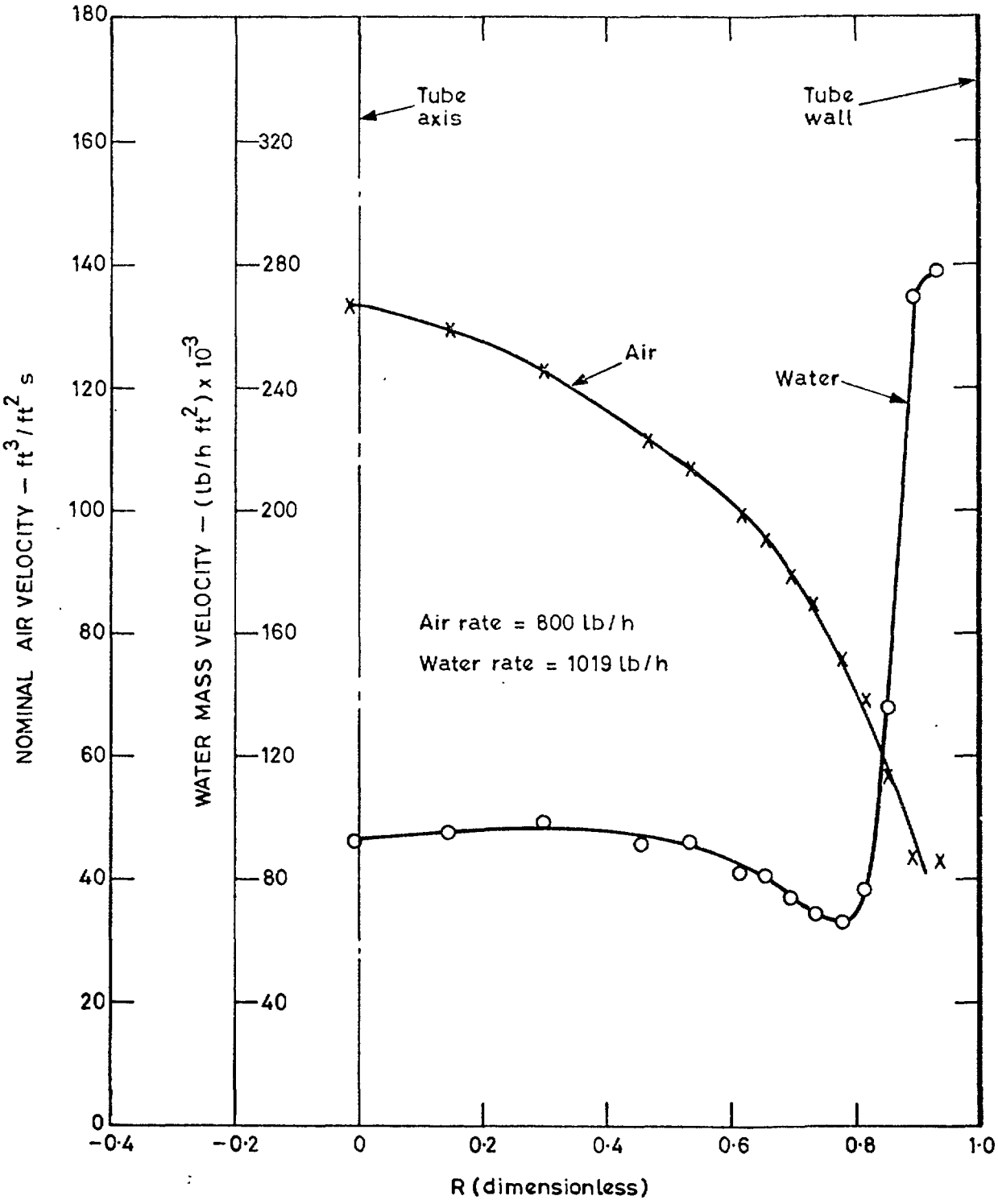

Fig 6. Mass velocity profiles obtained by the use of the isokinetic sampling prob. Data by Cousins and Hewitt (reproduced from ref [13] by permission). The liquid mass velocity shows a minimum in the vicinity of the interface.

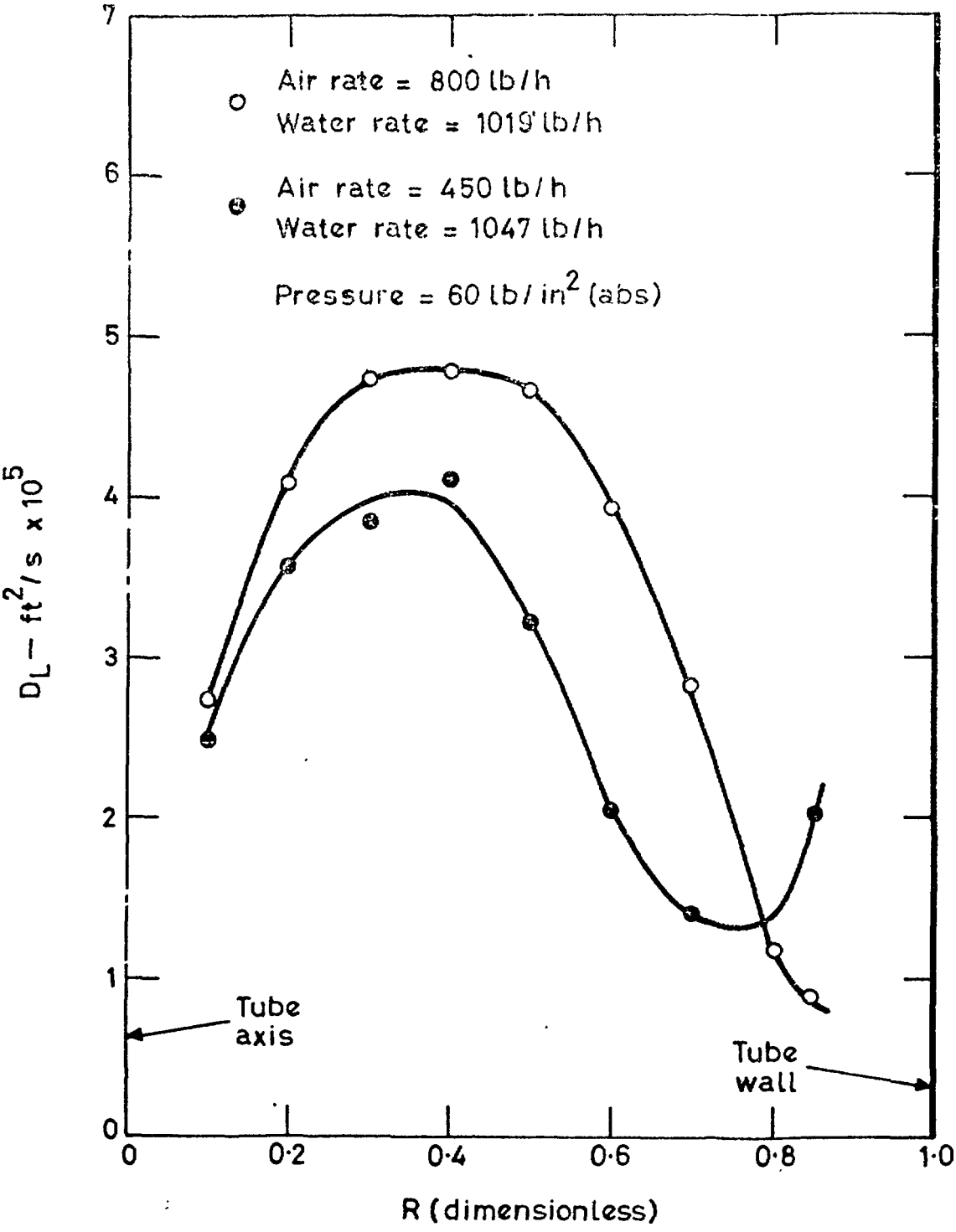

Fig 7. Dye diffusion coefficients measured across the channel. Data by Cousine and Hewitt (reproduced from ref [13] by permission).

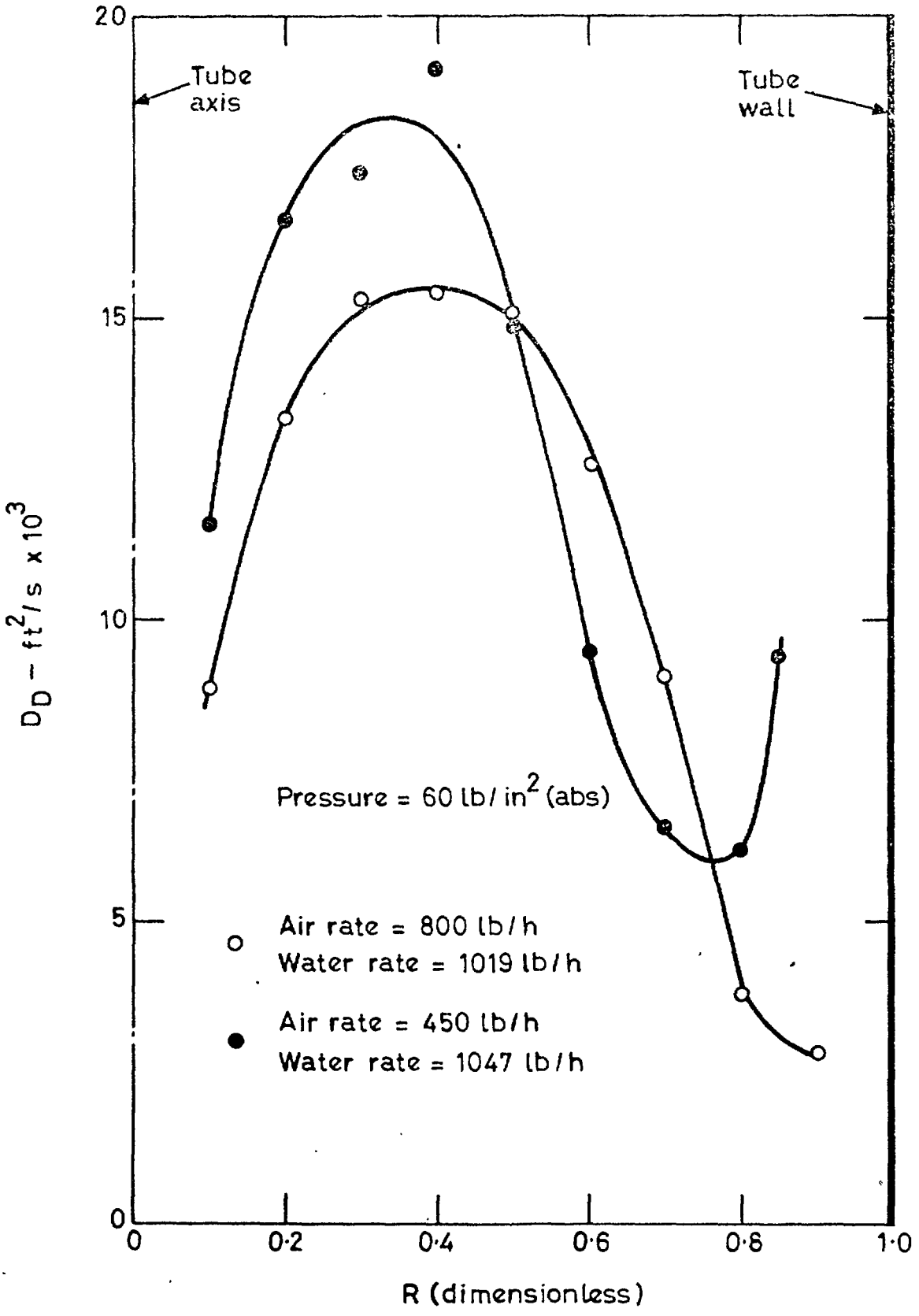

Fig 8. Dye diffusion coefficient measured across the channel. Data by Cousine and Hewitt (reproduced from ref [13] by permission).

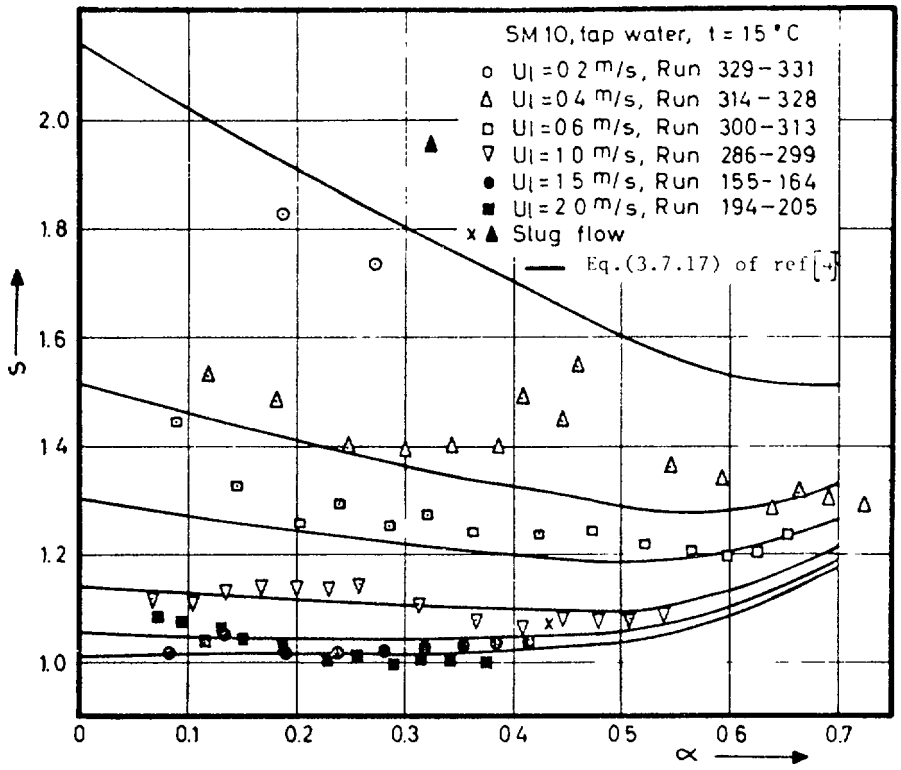

SLIP RATIOS IN 26,3 mm TUBE

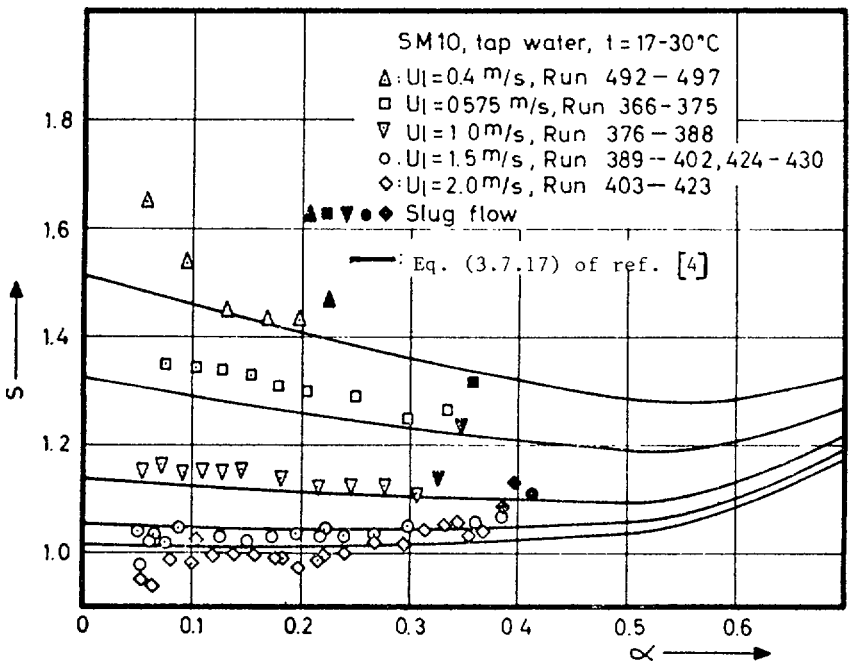

SLIP RATIOS IN 39,5 mm TUBE

Fig 9. Demonstration of the effects of liquid velocity, average void and other parameters on slip ratio in vertical upward flow. Data reported by D Malnes. (Reproduced from ref [4] by permission.)

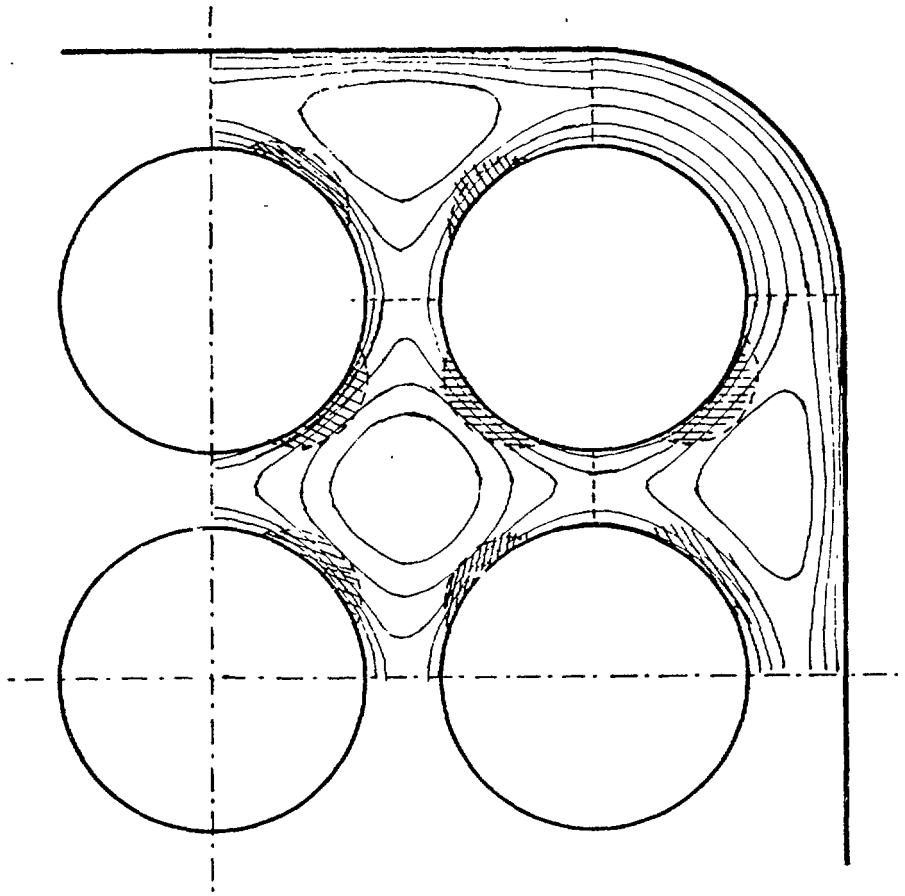

Zones of strong velocity gradients and intensive vortex rotation. (Bubble concentration.)

Fig 10. A sketch of the common subchannel types and the regions of bubble concentration in low quality boiling.

LIST OF PUBLISHED AE-REPORTS

1–420 (See back cover earlier reports.)

421. Decay curves and half-lives of gamma-emitting states from a study of prompt fission gamma radiation. By H. Albinsson. 1971. 28 p. Sw. cr. 15:–.
422. Adjustment of neutron cross section data by a least square fit of calculated quantities to experimental results. Part 1. Theory By H. Häggblom. 1971. 28 p. Sw. cr. 15:–.
423. Personnel dosimetry at AB Atomenergi during 1969. By J. Carlsson and T. Wahlberg. 1971. 10 p. Sw. cr. 15:–.
424. Some elements of equilibrium diagrams for systems of iron with water above 100°C and with simple chloride, carbonate and sulfate melts. By D. Lewis. 1971. 40 p. Sw. cr. 15:–.
425. A study of material buckling in uranium-loaded assemblies of the fast reactor FR0. By R. Håkansson and L. I. Tirén. 1971. 32 p. Sw. cr. 15:–.
426. Dislocation line tensions in the noble metals, the alkali metals and β-Brass. By B. Pettersson and K. Malén 1971. 14 p. Sw. cr. 15:–.
427. Studies of fine structure in the flux distribution due to the heterogeneity in some FR0 cores. By T. L. Andersson and H. Häggblom. 1971. 32 p Sw. cr. 15:–.
428. Integral measurement of fission-product reactivity worths in some fast reactor spectra. By T. L. Andersson. 1971. 36 p. Sw. cr. 15:–.
429. Neutron energy spectra from neutron induced fission of ^{235}U at 0.95 MeV and of ^{238}U at 1.35 and 2.02 MeV. By E. Almén, B. Holmqvist and T. Wiedling. 1971. 16 p. Sw. cr. 15:–.
430. Optical model analyses of experimental fast neutron elastic scattering data. By B. Holmqvist and T. Wiedling. 1971. 238 p. Sw. cr. 20:–.
431. Theoretical studies of aqueous systems above 25°C. 1. Fundamental concepts for equilibrium diagrams and some general features of the water system. By Derek Lewis. 1971. 27 p. Sw. cr. 15:–.
432. Theoretical studies of aqueous systems above 25°C . 2. The iron – water system. By Derek Lewis. 1971. 41 p. Sw. cr. 15:–.
433. A detector for (n,γ) cross section measurements. By J Hellström and S. Beshai. 1971. 22 p. Sw. cr. 15:–.
434. Influence of elastic anisotropy on extended dislocation nodes. By B. Pettersson. 1971. 27 p. Sw cr. 15:–.
435. Lattice dynamics of CsBr. By S. Rolandson and G. Raunio. 1971. 24 p. Sw. cr. 15:–.
436. The hydrolysis of iron (III) and iron (II) ions between 25°C and 375°C. By Derek Lewis. 1971.16 p. Sw. cr. 15:–.
437. Studies of the tendency of intergranular corrosion cracking of austenitic Fe-Cr-Ni alloys in high purity water at 300°C. By W. Hübner, B. Johansson and M. de Pourbaix. 1971. 30 p. Sw. cr. 15:–.
438. Studies concerning water-surface deposits in recovery boilers. By O. Strandberg, J. Arvesen and L. Dahl. 1971. 132 p. Sw. cr. 15:–.
439. Adjustment of neutron cross section data by a least square fit of calculated quantities to experimental results. Part II. Numerical results. By H. Häggblom. 1971 70 p. Sw. cr. 15:–.
440. Self-powered neutron and gamma detectors for in-core measurements. By O. Strindehag. 1971. 16 p. Sw cr. 15:–.
441. Neutron capture gamma ray cross sections for Ta, Ag, In and Au between 30 and 175 keV. By J. Hellström and S. Beshai. 1971. 30 p. Sw. cr. 15:–.
442. Thermodynamical properties of the solidified rare gases By I. Ebbsjö. 1971. 46 p. Sw. cr. 15:–.
443. Fast neutron radiative capture cross sections for some important standards from 30 keV to 1.5 MeV. By J. Hellström. 1971. 22 p. Sw. cr. 15:–.
444. A Ge (Li) bore hole probe for in situ gamma ray spectrometry. By A. Lauber and O. Landström. 1971 26 p. Sw cr 15:–
445. Neutron inelastic scattering study of liquid argon. By K. Sköld, J M. Rowe, G. Ostrowski and P. D. Randolph. 1972. 62 p. Sw. cr. 15:–.
446. Personnel dosimetry at Studsvik during 1970. By L. Hedlin and C.-O. Widell. 1972.. 8 p Sw. cr. 15:–.
447. On the action of a rotating magnetic field on a conducting liquid. By E. Dahlberg. 1972. 60 p. Sw. cr. 15:–.
448. Low grade heat from thermal electricity production. Quantity, worth and possible utilisation in Sweden By J. Christensen. 1972. 102 p. Sw cr. 15:–.
449. Personnel dosimetry at studsvik during 1971. By L. Hedlin and C.-O. Widell. 1972. 8 p. Sw. cr. 15:–.
450. Deposition of aerosol particles in electrically charged membrane filters By L. Ström. 1972. 60 p. Sw. cr. 15:–.
451. Depth distribution studies of carbon in steel surfaces by means of charged particle activation analysis with an account of heat and diffusion effects in the sample. By D. Brune, J. Lorenzen and E. Witalis. 1972. 46 p. Sw. cr. 15:–.
452. Fast neutron elastic scattering experiments. By M Salama. 1972. 98 p. Sw. cr. 15:–.
453. Progress report 1971 Nuclear chemistry. 1972. 21 p. Sw. cr. 15:–.
454. Measurement of bone mineral content using radiation sources. An annotated bibliography. By P. Schmeling. 1972. 64 p. Sw. cr. 15:–.
454. Measurement of bone mineral content using radiation sources. An annotated bibliography. Suppl. 1. By P. Schmeling. 1974. 26 p. Sw. cr. 20:–.
455. Long-term test of self-powered deectors in HBWR. By M. Brakas, O. Strindehag and B. Söderlund. 24 p. 1972. Sw. cr. 15:–.
456. Measurement of the effective delayed neutron fraction in three different FR0-cores. By L. Moberg and J. Kockum. 1972. Sw. cr. 15:–.
457. Applications of magnetohydrodynamics in the metal industry. By T. Robinson, J. Braun and S. Linder. 1972. 42 p. Sw. cr. 15:–.
458. Accuracy and precision studies of a radiochemical multielement method for activation analysis in the field of life sciences. By K. Samsahl. 1972. 20 p. Sw. cr. 15:–.
459. Temperature increments from deposits on heat transfer surfaces: the thermal resistivity and thermal conductivity of deposits of magnetite, calcium hydroxy apatite, humus and copper oxides. By T. Kelén and J. Arvesen. 1972. 68 p. Sw. cr. 15:–.
460. Ionization of a high-pressure gas flow in a longitudinal discharge. By S. Palmgren. 1972. 20 p. Sw. cr. 15:–.
461. The caustic stress corrosion cracking of alloyed steels – an electrochemical study. By L. Dahl, T. Dahlgren and N. Lagmyr. 1972. 43 p. Sw. cr. 15:–.
462. Electrodeposition of "point" $Cu^{125}I$ roentgen sources. By P. Beronius, B. Johansson and R. Söremark. 1972. 12 p. Sw. cr. 15:–.
463. A twin large-area proportional flow counter for the assay of plutonium in human lungs. By R. C. Sharma, I. Nilsson and L. Lindgren. 1972. 50 p. Sw cr. 15:–.
464. Measurements and analysis of gamma heating in the R2 core. By R. Carlsson and L. G. Larsson. 1972. 34 p. Sw. cr. 15:–.
465. Determination of oxygen in zircaloy surfaces by means of charged particle activation analysis. By J. Lorenzen and D. Brune. 1972. 18 p. Sw. cr. 15:–.
466. Neutron activation of liquid samples at low temperature in reactors with Reference to nuclear chemistry. By D. Brune. 1972. 8 p. Sw. cr. 15:–.
467. Irradiation facilities for coated particle fuel testing in the Studsvik R2 reactor. By S. Sandklef. 1973. 28 p. Sw. cr. 20:–.
468. Neutron absorber techniques developed in the Studsvik R2 reactor. By R. Bodh and S. Sandklef. 1973. 26 p. Sw cr. 20:–.
469. A radiochemical machine for the analysis of Cd, Cr, Cu, Mo and Zn. By K. Samsahl, P. O. Wester, G. Blomqvist. 1973. 13 p. Sw. cr. 20:–.
470. Proton pulse radiolysis. By H. C. Christensen, G. Nilsson, T. Reitberger and K.-Å. Thuomas. 1973. 26 p. Sw. cr. 20:–.
471. Progress report 1972. Nuclear chemistry. 1973. 28 p. Sw. cr. 20:–.
472. An automatic sampling station for fission gas analysis. By S. Sandklef and P.Svensson 1973. 52 p. Sw. cr. 20:–.
473. Selective step scanning: a simple means of automating the Philips diffractometer for studies of line profiles and residual stress. By A. Brown and S. Å. Lindh. 1973. 38 p. Sw. cr. 20:–.
474. Radiation damage in CaF_2 and BaF_2 investigated by the channeling technique By R. Hellborg and G. Skog. 1973. 38 p. Sw. cr. 20:–.
475. A survey of applied instrument systems for use with light water reactor-containments. By H. Tuxen-Meyer. 1973. 20 p. Sw. cr. 20:–.
476. Excitation functions for charged particle induced reactions in light elements at low projectile energies. By J. Lorenzen and D. Brune. 1973. 154 p. Sw. cr. 20:–.
477. Studies of redox equilibria at elevated temperatures 3. Oxide/oxide and oxide/metal couples of iron, nickel, copper, silver, mercury and antimony in aqueous systems up to 100°C. By Karin Johansson, Kerstin Johnsson and Derek Lewis. 1973. 42 p. Sw. cr. 20:–.
478. Irradiation facilities for LWR fuel testing in the Studsvik R2 reactor. By S. Sandklef and H. Tomani. 1973. 30 p. Sw. cr. 20:–.
479. Systematics in the (p,xn) and (p,pxn) reaction cross sections. By L. Jéki. 1973. 14 p. Sw. cr. 20:–.
480. Axial and transverse momentum balance in subchannel analysis. By S. Z. Rouhani. 1973. 58 p. Sw. cr. 20:–.
481. Neutron inelastic scattering cross sections in the energy range 2 to 4.5 MeV. Measurements and calculations. By M. A. Etemad. 1973. 62 p. Sw. cr. 20:–.
482. Neutron elastic scattering measurements at 7.0 MeV. By M. A. Etemad. 1973. 28 p. Sw. cr. 20:–.
483. Zooplankton in Tvären 1961–1963. By E. Almquist. 1973. 50 p. Sw. cr. 20:–.
484. Neutron radiography at the Studsvik R2-0 reactor. By I. Gustafsson and E. Sokolowski. 1974. 54 p. Sw. cr. 20:–.
485. Optical model calculations of fast neutron elastic scattering cross sections for some reactor materials. By M. A. Etemad. 1974. 165 p. Sw. cr. 20:–.
486. High cycle fatigue crack growth of two zirconium alloys. By V. S. Rao. 1974. 30 p. Sw. cr 20:–.
487. Studies of turbulent flow parallel to a rod bundle of triangular array. By B. Kjellström. 1974. 190 p. Sw. cr. 20:–.
488. A critical analysis of the ring expansion test on zircaloy cladding tubes. By K. Pettersson. 1974. 8 p. Sw. cr. 20:–.
489. Bone mineral determinations. Proceedings of the symposium on bone mineral determinations held in Stockholm-Studsvik, Sweden, 27-29 may 1974 vol. 3. Bibliography on bone morphometry and densitometry in man. By A. Horsman and M. Simpson. 1974. 112 p. Sw. cr. 20:–.
490. The over-power ramp fuel failure phenomenon and its burn-up dependence – need of systematic, relevant and accurate irradiation investigations. – Program proposal. By Hilding Mogard. 1974. Sw. cr. 20:–.
491. Phonon Anharmonicity of Germanium in the Temperature Range 80–880 K. By G. Nelin and G. Nilsson. 1974. 28 p. Sw. cr. 20:–.
492. Harmonic Lattice Dynamics of Germanium. By G. Nelin. 1974. 32 p. Sw. cr. 20:–.
493. Diffusion of Hydrogen in the β-Phase of Pd-H Studied by Small Energy Transfer Neutron Scattering. By G. Nelin and K. Sköld. 1974. 28 p. Sw. cr. 20:–.
495. Estimation of the rate of sensitization in nickel base alloys.By J. Wiberg. 1974. 14 p. Sw. cr. 20:–.
497. Effect of wall friction and vortex generation on radial void distribution – the wall-vortex effect. By Z. Rouhani. 1974. 36 p. Sw. cr. 20:–.

List of published AES-reports (In Swedish)

1. Analysis by means of gamma spectrometry. By D. Brune. 1961. 10 p. Sw. cr. 6:–.
2. Irradiation changes and neutron atmosphere in reactor pressure vessels-some points of view. By M. Grounes. 1962. 33 p. Sw cr. 6:–.
3. Study of the elongation limit in mild steel. By G. Östberg and R. Attermo. 1963. 17 p. Sw. cr. 6:–.
4. Technical purchasing in the reactor field. By Erik Jonson. 1963. 64 p. Sw. cr. 8:–.
5. Ägesta nuclear power station. Summary of technical data, descriptions, etc. for the reactor. By B. Lilliehöök. 1964. 336 p. Sw. cr. 15:–
6. Atom Day 1965. Summary of lectures and discussions. By S. Sandström. 1966. 321 p. Sw. cr. 15:–.
7. Building materials containing radium considered from the radiation protection point of view. By Stig O. W. Bergström and Tor Wahlberg. 1967. 26 p. Sw. cr. 10:–.
8. Uranium market. 1971. 30 p. Sw. cr. 15:–.
9. Radiography day at Studsvik. Tuesday 27 april 1971. Arranged by AB Atomenergy, IVA's Committee for nondestructive testing and TRC AB. 1971. 102 p. Sw. cr. 15:–.
10. The supply of enriched uranium. By M. Mårtensson. 1972. 53 p. Sw. cr. 15:–.
11. Fire studies of plastic-insulated electric cables, sealing lead-in wires and switch gear cubicles and floors. 1973. 117 p. Sw. cr. 35:–.

Additional copies available from the Library of AB Atomenergi, Fack, S-611 01 Nyköping 1, Sweden.

EOS-tryckerierna, Stockholm 1974